Vol. 136: 87–103, 2019
https://doi.org/10.3354/dao03417

DISEASES OF AQUATIC ORGANISMS
Dis Aquat Org

Published online October 2

Contribution to DAO Special 8 'Amphipod disease: model systems, invasions and systematics'

Ultrastructure, phylogeny and histopathology of two novel haplosporidians parasitising amphipods, and importance of crustaceans as hosts

Ander Urrutia[1,2], David Bass[1,3,*], Georgia Ward[1,3], Stuart Ross[1], Jamie Bojko[4], Ionan Marigomez[2], Stephen W. Feist[1]

[1]Centre for Environment, Fisheries, and Aquaculture Science (Cefas), Barrack Road, The Nothe, Weymouth, Dorset DT4 8UB,UK

[2]Department of Zoology and Animal Cell Biology, Science and Technology Faculty and Research Centre for Experimental Marine Biology and Biotechnology (PIE-UPV/EHU), University of the Basque Country (UPV/EHU), PO Box 644, 48080 Bilbao, Basque Country, Spain

[3]Department of Life Sciences, The Natural History Museum, Cromwell Road, London SW7 5BD, UK

[4]School of Forest Resources and Conservation, Program in Fisheries and Aquatic Sciences, and Emerging Pathogens Institute, University of Florida, Gainesville, FL 32611, USA

ABSTRACT: This study provides morphological, ultrastructural and phylogenetic characterization of 2 novel species of the order Haplosporida (*Haplosporidium echinogammari* n. sp. and *H. orchestiae* n. sp.) infecting amphipods of the genera *Echinogammarus* and *Orchestia* collected in southwestern England. Both parasites infect the connective tissues associated with the digestive gland and the tegument, and eventually infect other organs causing disruption of host tissues with associated motor impairment and fitness reduction. Prevalence of infection varied with host species, provenance and season, being as high as 75% for individuals of *E. marinus* infected with *H. echinogammari* in June (n = 50). Although no spores were found in any of the infected amphipods examined (n = 82), the morphology of monokaryotic and dikaryotic unicellular stages of the parasites enabled differentiation between the 2 new species. Phylogenetic analysis of the new species based on the small subunit (SSU) rDNA gene placed *H. echinogammari* close to *H. diporeiae* in haplosporidian lineage C, and *H. orchestiae* in a novel branch within *Haplosporidium*. An additional 25 new haplosporidian SSU rDNA sequences were generated from crab, isopod, and crayfish samples, significantly increasing the number of crustacean-derived sequences within Haplosporida, which was previously thought to comprise mostly parasites of molluscs. Phylogenetic analysis of these new sequences revealed 3 clades of primarily crustacean-derived sequences within Haplosporida.

KEY WORDS: *Echinogammarus* · *Orchestia* · Crustacea · *Haplosporidium echinogammari* · *Haplosporidium orchestiae* · Host–parasite association · Life cycle · Phylogeny

1. INTRODUCTION

The Order Haplosporida (Caullery & Mesnil 1899), within the Class Ascetosporea (Sub-phylum Endomyxa), comprises 4 genera (*Minchinia, Bonamia, Urosporidium* and *Haplosporidium*), all small endoparasites of marine and freshwater invertebrates (Hartikainen et al. 2014). Several species within the clade are well known parasites of bivalves, causing recurrent mortality events (Haskin & Andrews 1988) that decimate natural and farmed populations (Ford & Figueras 1988). Notorious examples of substantial economic losses associated with haplosporidian infections include the decline of eastern oyster *Crass-*

*Corresponding author: david.bass@cefas.co.uk

Publisher: Inter-Research · www.int-res.com

ostrea virginica populations on the east coast of North America due to *H. nelsoni* (MSX disease) and *H. costale* (Ford & Tripp 1996). Infection with *Bonamia ostreae* was a major factor associated with the collapse of *Ostrea edulis* production in Europe in the last decades of the 20th century (Pichot et al. 1979, Friedman & Perkins 1994). In contrast to economic losses affecting aquaculture, the ecological significance of haplosporidian infections is more difficult to determine. However, there is significant evidence of the impact of haplosporidians on non-cultured species from a wide range of environments. Infection with *H. pinnae* appears to be a key factor in the decline of the fan mussel *Pinna nobilis* in the Mediterranean Sea (Trigos et al. 2014, Catanese et al. 2018). In addition, there may be reduced bioturbation of sediments as a consequence of polychaetes becoming infected by *H. parisi* and *H. scolopli* (Ormières 1980, Paramor & Hughes 2004), or even changes in the population structure of important invertebrate predators such as the common shore crab *Carcinus maenas* infected by *H. littoralis* (Stentiford et al. 2013).

The taxonomic relationships within the Order Haplosporida remain a challenge more than a century after its discovery. Currently, there are approximately 54 described haplosporidian species, with approximately 20 unnamed organisms and at least another 50 uncharacterized sequences distributed within or related to 1 of the 4 genera constituting the Order Haplosporida. Despite advances in the understanding of the phylogeny of the group following the introduction of electron microscopy in the 1950s and molecular techniques in the last 25 yr (Cavalier-Smith 1993, Berthe et al. 2000, Hartikainen et al. 2014), aspects of the life cycle, diversity, ecology and even morphological features remain poorly understood. Haplosporida are parasitic protists having multinucleate plasmodia and ovoid-walled spores lacking a polar filament and with an orifice at one pole (Perkins 2000). Historically, divisions between genera have been based on spore ornamentation. *Urosporidium* is clearly distinguished from the others by having an internal flap of wall material covering the orifice of the spore. Morphological differentiation between *Minchinia* and *Haplosporidium*, both with an external hinged lid, proved more difficult due to failure to find new comparative type material of both genera, which were described in the early 20th century. In addition, the presence of apparently non-spore-forming *Bonamia* in the order muddied the description until the first spore-forming *Bonamia* sp. was found (Carnegie et al. 2006). Ormières (1980) proposed separating *Minchinia* and *Haplosporidium*, based on the origin of the spore ornamentation. Spore ornamentation composed of epispore cytoplasm would define the genus *Minchinia*, while spore-wall formed ornamentation would define the genus *Haplosporidium*. Molecular analyses (Reece et al. 2004) support this ontogenic hypothesis and confirm the monophyly of *Urosporidium*, *Bonamia* and *Minchinia*. However, *Haplosporidium* is currently paraphyletic, highlighting the need for taxonomic revisions based on molecular characterizations, histopathological and ultrastructural descriptions to facilitate the erection of novel monophyletic genera (Burreson & Ford 2004, Hartikainen et al. 2014, Ward et al. 2018). Attention is increasingly being focussed on haplosporidian infections in non-molluscan invertebrates, including crabs and amphipods, as definitive or intermediate hosts.

Amphipoda is a major order of ubiquitous malacostracan crustaceans, characterized by the lack of carapace, differentiated limbs or 'poda' and a mediolateral flattening of the body. The adaptability, resilience to abiotic fluctuations and wide spectrum of feeding strategies developed by these benthic crustaceans have allowed them to colonize some of the most demanding and hostile environments, including polar regions (Poltermann 2001) and hydrothermal vents (Sheader et al. 2004). With almost 10 000 species, mainly in marine ecosystems, the role played by scavenging and detritivorous amphipods as secondary producers (Norderhaug & Christie 2011), decomposing and recycling organic matter back to the food web (Wilson & Wolkovich 2011), makes them a dominant component of many benthic macroinvertebrate assemblages (MacNeil et al. 1997). Predictably, being extremely abundant in a wide range of ecosystems makes amphipods an important part of the diet for other crustaceans, fish, birds and even mammals (Garrison & Link 2000, Bocher et al. 2001, Holst et al. 2001). They are also used as a protein source in aquaculture (Moren et al. 2007). In addition to their diversity, abundance and ecological importance, amphipods are widely used in biomonitoring (Fialkowski et al. 2003) and toxicological studies (Hanna et al. 2013). Yet, there is a notable lack of information and understanding of amphipods as vectors, reservoirs and primary hosts for a number of parasites.

Although molluscs are the best-known hosts of haplosporidian parasites, awareness of the role played by crustacean hosts has increased in recent decades (Hine et al. 2009). Some of these relationships potentially have ecological and commercial importance, as

haplosporidians infect several species of crabs (Stentiford et al. 2013) and shrimps (Bower & Meyer 2002, Utari et al. 2012). However, there is very limited information on Haplosporida infecting amphipods. The first of these to be described, *H. gammari* (later reclassified as *Claustrosporidium gammari* due to the lack of pore in the spore; Larsson 1987), infected *Rivulogammarus pulex* sampled near Louvain in Belgium (Van Ryckeghem 1930). It took some 50 yr before another infected *R. pulex* was studied (Larsson 1987), and there are no gene sequences for this parasite. More recent discoveries include *H. diporeiae* infecting the benthic amphipod *Diporeia* sp. in the Laurentian Great Lakes in the USA (Winters & Faisal 2014) and haplosporidian-like parasites infecting *Parhyale hawaiensis* collected from Sharm El-Nagha, on the Egyptian coast of the Red Sea (Ismail 2011). Ecological implications of haplosporidians infecting amphipods have been proposed in a recent study (Cave & Strychar 2015), suggesting a potential association between *H. diporeiae* infection and amphipod population declines in the Great Lakes since the late 1980s (Nalepa et al. 2007).

In this study, we describe the infection of amphipods by 2 novel species of *Haplosporidium*. The first species was found infecting amphipods of the genus *Orchestia* collected from Tamar and Dart estuaries (southwestern UK), and Butrón estuary, in northern Spain. The second species was detected in *Echinogammarus marinus* sampled from Newton's Cove (Weymouth, UK). We provide histological, ultrastructural and phylogenetic information for both new species.

2. MATERIALS AND METHODS

2.1. Sample collection

Amphipods belonging to the genera *Orchestia* and *Echinogammarus* were collected from the Dart Estuary (Dittisham, Devon, UK), Newton's Cove (Weymouth, Dorset, UK), and the Butrón estuary (Plentzia, Spain) in 2016 and 2017, as shown in Table 1. Amphipods of the genera *Gammarus* and *Pontogammarus* were sampled in Poland as described in Bojko (2017).

2.2. Histology and transmission electron microscopy

Amphipods were kept alive and dissected within 3–4 h post collection. The head and anterior part of the thorax were immediately fixed in 100% molecular grade ethanol. The proximate segments of the thorax of about 2 mm in size were placed in 2.5% glutaraldehyde in 0.1 M sodium cacodylate buffer (pH 7.4) for electron microscopy. The remainder of the body, which included the last 3–4 segments of the pereon and the pleon, were fixed in Davidson's seawater fixative (Hopwood 1996) for 24 h, then transferred to 70% ethanol.

For histology, Davidson's fixed samples were processed from ethanol to wax in a vacuum infiltration processor using established laboratory protocols (Stentiford et al. 2013). Tissue sections were cut at a thickness of 2.5–3 µm on a Finnese® microtome, left to dry for 24 h after mounting on VWR™ microscope slides and stained with H&E (Bancroft & Cook 1994). Cover-slipped sections were examined for general histopathology by light microscopy (Nikon Eclipse E800). Digital images and measurements were obtained using the Lucia™ Screen Measurement software system (Nikon). Measurements of unicellular parasite stages were performed only for those showing good fixation and clear structure and for plasmodia which were not compressed by adjacent host tissues. Statistical analysis for normality and comparison between measurements was conducted in RStudio™. The level of infection was assessed using a scale ranging from 1 to 4 (1: few parasite cells infecting few host tissues; 2: unicellular and plasmodial stages in haemolymph and tegument; 3: several organs and connective around them affected; and 4: systemic infection often associated with important tissue disruption).

Four amphipod samples showing haplosporidian infections by light microscopy were selected for transmission electron microscopy (TEM) analysis. Glutaraldehyde-fixed samples were rinsed in 0.1 M sodium cacodylate buffer (pH 7.4) and post-fixed for 1 h in 1% osmium tetroxide in 0.1 M sodium cacodylate buffer. Samples were washed in 3 changes of 0.1 M sodium cacodylate buffer before dehydration through a graded acetone series. Samples were embedded in epoxy resin 812 (Agar Scientific pre-Mix Kit 812) and polymerised overnight at 60°C. Semi-thin (1 µm) sections were stained with 1% Toluidine Blue and examined under a light microscope to identify target areas containing sufficient parasites. Ultrathin sections (70–90 nm) were framed on uncoated copper grids and stained with uranyl acetate and Reynold's lead citrate (Reynolds 1963). Grids were examined using a JEOL JEM 1400 transmission electron microscope,

Table 1. Sampling information for the amphipod species collected in this study (Polish samples are from Bojko 2017). Specific coordinates are provided for the exact sampling site together with the locality and the habitat (environment)

Sampling site	Locality	Environment	Niche	Date	Taxon	n	Coordinates
Newton's Cove	Weymouth, UK	Marine water	Upper shore, underneath rocks	April 2016 to Dec 2017	*E. marinus*	30 (per month)	50° 36′ 17″ N, 02° 27′ 03′ W
Dart estuary	Dittisham, UK	Brackish water	Upper shore, underneath rocks	27 Apr 2017	*Orchestia* sp.	30	50° 23′ 21″ N, 03° 35′ 36″ W
Dart estuary	Dittisham, UK	Brackish water	Upper shore, underneath rocks	27 Apr 2017	*E. marinus*	30	50° 23′ 21″ N, 03° 35′ 36″ W
Butrón estuary	Plentzia, Spain	Brackish water	Upper shore, underneath rocks	30 Aug 2017	*Orchestia* sp.	30	43° 24′ 25″ N, 02° 57′ 23″ W
Oder river	Gryfino, Poland	Fresh water	Water column/sediment on the embankment	23 Jun 2015	*Pontogammarus robustoides*	122	53° 15′ 09″ N, 14° 26′ 53″ E
Bug river	Porçba-Kocęby, Poland	Fresh water	Water column/sediment on the embankment	21 Jun 2015	*Gammarus varsoviensis*	109	52° 41′ 28″ N, 21° 41′ 12″ E

and digital images were captured using a GATAN Erlangshen ES500W camera and Gatan Digital Micrograph™ software.

2.3. DNA extraction, PCR and sequencing

Amphipod gonad, gill, muscle, connective tegumental, nervous and digestive tissues were preserved in 100% molecular grade ethanol (Fisher BioReagents™). Samples found to be infected via histology were selected for DNA extraction, PCR amplification and sequencing. Infected tissues were disrupted and digested overnight using Fast Prep® Lysing Matrix tubes containing 0.2 mg (6 U) Proteinase K (Sigma-Aldrich®) diluted 1/40 in Lifton's buffer (100 mM EDTA, 25 mM Tris-HCl, 1% [v/v] SDS, pH 7.6). The following day, 1/10 (v/v) of 5 M potassium acetate was added, and tubes were incubated on ice for 1 h. From here, DNA was extracted using the phenol–chloroform method described by Chomczynski & Sacchi (1987). Partial small subunit (SSU) rDNA gene sequences belonging to the different haplosporidians were amplified by PCR as follows; the total reaction volume of 50 µl included 30.75 µl molecular water, 10 µl GoTaq® Flexi Buffer, 2.0 mM $MgCl_2$, 0.2 mm of each deoxyribonucleotide, 40 pM of each primer, 1.25 U GoTaq® Polymerase (Promega) and 200 ng of DNA. Cycling parameters were 3 min of denaturation at 95°C; followed by 35 cycles of 95°C (30 s), annealing (1 min) at 65°C and extension (1 min) at 72°C; with extension final. Amplicons were at 72°C (10 mins) and stored at 4°C. Primers (Table 2), conditions and concentrations used for nested PCR followed Hartikainen et al. (2014). The resulting band (650 bp) was dissected and cleaned using 20% polyethylene glycol 8000 (Sigma-Aldrich®) solution. A total volume of 15 µl of purified DNA with a concentration of (5 ng μl^{-1}) was mixed with 2 µl (10 µM) of forward primer (V5fHapl) and single-read Sanger sequenced (Eurofins®Genomics).

2.4. Sequence alignment and phylogenetic analysis

Haplosporidian sequences were confirmed by BlastN searches (Zhang et al. 2000) against the GenBank nt database and by constructing preliminary trees. Sanger sequence chromatograms were edited by eye, and potentially aberrant nucleotides in highly conserved regions were replaced by an 'N' when their quality scores were lower than Q30. Reference sequences from a comprehensive haplosporidian dataset (Hartikainen et al. 2014) were downloaded and aligned with our own sequences in MAFFT (Katoh et al. 2017) using the L-ins-i algorithm, and the following parameters: 200 PAM/K=2 scoring matrix, 1.53 GAP opening penalty, with N having no effect on the alignment score. Sequences belonging

Table 2. Primers used for haplosporidian PCR amplification, as in Hartikainen et al. (2014). SSU: small subunit

Primer	Sequence	Specificity
C5fHapl	5′-GTA GTC CCA RCY ATA AAC BAT GTC-3′	Haplosporidia SSU
Sb1n	3′-GAT CCH TCY GCA GGT TCA CCT ACG-5′	Universal eukaryote
V5fHapl	5′-GGA CTC RGG GGG AAG TAT GCT-3′	Haplosporidian SSU
Sb2nHap	3′-CCT TGT TAC GAC TTB TYC TTC CTC-5′	Eukaryote (Haplosporida-biased)

to haplosporidian parasites deposited in GenBank after 2014 were also added. The alignment was edited in MEGA v7.0 (Kumar et al. 2016), and ragged ends were cropped. Final refinement of the alignment was manually curated in Aliview (Larsson 2014). A maximum likelihood (ML) phylogenetic tree was constructed using RAxML Blackbox (GTR model with CAT approximation (all parameters estimated from the data); averages of 402 bootstrap values (MRE-based bootstopping criterion) were mapped onto the tree with the highest likelihood value (evaluated under GAMMA) (Kozlov et al. 2019) on the Cipres Science Gateway (Miller et al. 2010). A Bayesian inference consensus tree was built using MrBayes v.3.2 (Ronquist et al. 2012) on Cipres using default likelihood model parameters except for the following changes: the number of substitution types was mixed; model for among-site rate variation, Invgamma; use of covarion like model, activated; MCMC parameters: 5 million generations and all compatible groups consensus tree. A final consensus tree was created on FigTree v1.4 (Rambaut 2014) based on the Bayesian topology. Following the same procedure, a second tree with different taxon sampling was generated including an additional 25 newly generated parasite sequences associated with crustacean hosts obtained from archive material from other projects, using the same PCR and analytical protocols as described above. No histological data were available for these 25 sequences.

3. RESULTS

3.1. Clinical signs and prevalence

Haplosporidian infections in heavily infected *Echinogammarus marinus* and *Orchestia* sp. were suggested macroscopically by whitish and opaque colouration of the body. Infection was also often associated with reduced jumping ability in the genus *Orchestia* and lethargic behaviour in *E. marinus*. When dissected, the haemolymph of severely infected individuals was more viscous and cloudier than that of uninfected individuals. Haplosporidiosis in *E. marinus* showed a distinct peak in prevalence during June/July, whilst prevalence of haplosporidiosis in *Orchestia* sp. was high in April (Fig. 1). For haplosporidian parasites infecting *E. marinus* in other locations and other amphipod genera, prevalence varied with the location and time of the sampling (Fig. 1). Only 1 out of 107 (0.93%) individuals of *Gammarus varsoviensis* sampled from Western Bug in Porçba-Koceby showed a level of infection, while the prevalence was 3.2% for the haplosporidian infecting *Pontogammarus robustoides* (n = 122) in the Oder River as it passes near the town of Gryfino (Table 1) (Bojko 2017).

3.2. Histopathology and ultrastructure

Light microscopy revealed morphological differences between infections in different hosts and locations. No spore stages were found in any of the infected amphipods examined (n = 82). Significant differences in length and width of the unicellular stages suggested 2 clearly differentiated taxa (Table 3). TEM supported light microscopy observations, showing clear ultrastructural differences between the parasites in *E. marinus* and *Orchestia* sp. (Figs. 2 & 3).

In amphipod hosts with early haplosporidian infections, parasites were mainly located in the connective tissue, especially around intestine and hepatopancreas (Figs. 2A & 3A). The tegument was only lightly infected. During this phase of the infection, only plasmodial stages of the parasite were observed, most of them with fewer than 10 nuclei. As the intensity of infection increased, parasite stages were observed in the haemolymph (Figs. 2B & 3B), facilitating spread of infection throughout the body, with exception of the

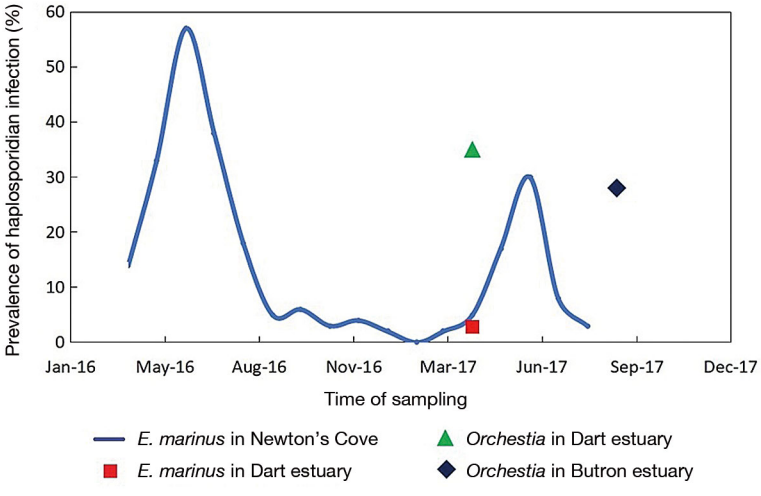

Fig. 1. Prevalence of haplosporidian infection for different times of the year and amphipod species. Blue line: prevalence in *Echinogammarus marinus* sampled in Newton's Cove from April 2016 to August 2017. Red square: prevalence in *E. marinus* sampled in Dart estuary (Dittisham), 27 April 2017. Green triangle: prevalence in *Orchestia* sp. sampled in Dart estuary, 27 April 2017. Blue diamond: prevalence in *Orchestia* sp. sampled in Butrón estuary, 30 August 2017

Table 3. Individual amphipod samples showing haplosporidian infection. The GenBank accession number links to the phylogenetic tree in Fig. 5. Information on the level of infection, tissues infected and parasite stage specificity for tissues can be found under 'Histopathology', and morphometric measurements (mean ± SD) of the plasmodial and unicellular stages are shown under 'Parasite morphology'(L: length; W: width; nd: no data—not measureable; np: not present). Paired *t*-test comparing the length of monokaryotic cells of *E. marinus* and *Orchestia* sp.: $p < 2.2 \times 10^{-16}$. Mann-Whitney *U*-test for the width of monokaryotic cells (non-normal distribution): $p < 2.2 \times 10^{-16}$. Paired *t*-test for the length of dikaryotic cells: $p = 1.48 \times 10^{-07}$. Paired *t*-test for the width of dikaryotic cells: $p < 2.2 \times 10^{-16}$

GenBank accession	Host			Histopathology				Parasite morphology		
	Species	Sampling location	Date	Level of infection	Tissues infected	Unicellular stages	Plasmodial stages	Plasmodium size (µm)	Monokaryotic stage size (µm)	Dikaryotic stage size (µm)
MK913658	*Echinogammarus marinus*	Newton's Cove (UK)	18 May 17	4	Tegument, connective and haemolymph	Haemolymph	Connective	7.14 ± 0.85	L: 2.56 ± 0.39 W: 1.79 ± 0.17	L: 4.25 ± 0.46 W: 1.38 ± 0.17
MK913659	*E. marinus*	Newton's Cove (UK)	18 May 17	4	Tegument, connective and haemolymph	Haemolymph	Connective	7.35 ± 1.00	L: 2.48 ± 0.29 W: 1.77 ± 0.24	L: 4.37 ± 0.48 W: 1.34 ± 0.15
MK913660	*E. marinus*	Newton's Cove (UK)	18 May 17	3	Mainly connective, especially around intestine and hepatopancreas, tegument	Absent	Connective and tegument	7.10 ± 0.76	–	–
MK913661	*E. marinus*	Newton's Cove (UK)	18 May 17	1	Connective tissue around intestine; few plasmodia present in tegument	Absent	Connective and tegument	7.52 ± 1.20	–	–
MK913670	*Pontogammarus robustoides*	Oder river (Gryfino, Poland)	23 Jun 15	3	Tegument and connective	Connective and tegument	Connective and tegument	7.11 ± 0.90	nd	nd
MK913664	*P. robustoides*	Oder river (Gryfino, Poland)	23 Jun 15	4	Connective, tegument and muscle	Absent	Connective, tegument and muscle	7.39 ± 0.95	–	–
MK913669	*P. robustoides*	Oder river (Gryfino, Poland)	23 Jun 15	3	Mainly connective, especially around gonads, intestine and hepatopancreas; tegument	Few unicellular stages, mainly in tegument	Connective and tegument	7.03 ± 1.05	nd	nd
MK913665	*Gammarus varsoviensis*	Bug river (Poręba Kocęby, Poland)	21 Jun 15	–	–	–	–	–	–	–
MK913663	*E. marinus*	Newton's Cove (UK)	08 Jun 16	3	Mainly connective, especially around gonads, intestine and hepatopancreas; tegument and haemolymph	Haemolymph, connective and tegument	Mainly connective	6.27 ± 0.81	L: 2.43 ± 0.24 W: 1.72 ± 0.19	L: 4.08 ± 0.55 W: 1.36 ± 0.16
MK913662	*E. marinus*	Newton's Cove (UK)	08 Jun 16	3	Connective, tegument, hepatopancreas and haemolymph (inside haemocytes)	Haemolymph and tegument	Connective and tegument	7.08 ± 1.08	L: 2.63 ± 0.42 W: 1.87 ± 0.28	L: 4.14 ± 0.45 W: 1.40 ± 0.16
MK913655	*E. marinus*	Newton's Cove (UK)	13 Sep 16	1	Connective, especially around intestine and hepatopancreas; few plasmodia in tegument	Absent	Mainly connective; tegument	6.32 ± 0.70	–	–
MK913657	*Gammarus* sp.	Newton's Cove (UK)	14 Dec 16	3	Connective around intestine and tegument; muscle also infected	Haemolymph and tegument	Connective	7.64 ± 1.31	L: 2.49 ± 0.27 W: 1.66 ± 0.16	np
MK913671	*E. marinus*	Newton's Cove (UK)	20 Apr 16	1	–	–	–	–	–	–
MK913656	*Orchestia* sp.	Butrón estuary (Spain)	30 Aug 17	4	Mainly haemolymph; connective, tegument and muscle	Mainly in haemolymph	Few plasmodia; connective	8.36 ± 1.28	L: 3.59 ± 0.22 W: 2.04 ± 0.22	L: 3.86 ± 0.40 W: 3.18 ± 0.33
MK913666	*Orchestia* sp.	Butrón estuary (Spain)	30 Aug 17	4	Mainly haemolymph; connective and tegument	Haemolymph and tegument	Connective around intestine and gonads; tegument	8.13 ± 1.12	L: 3.65 ± 0.38 W: 2.09 ± 0.19	L: 3.61 ± 0.35 W: 3.12 ± 0.32
MK913668	*Orchestia* sp.	Dart estuary (UK)	27 Apr 17	3	Tegument, connective and haemolymph	Haemolymph and tegument	Connective around intestine and gonads; tegument	9.24 ± 1.04	L: 3.63 ± 0.24 W: 2.00 ± 0.23	L: 3.80 ± 0.31 W: 3.13 ± 0.34
MK913667	*Orchestia* sp.	Dart estuary (UK)	27 Ap 17	4	Connective completely substituted; tegument and haemolymph	Haemolymph and tegument	Connective around intestine and gonads	9.59 ± 1.10	L: 3.49 ± 0.42 W: 2.15 ± 0.22	L: 4.22 ± 0.32 W: 3.04 ± 0.37

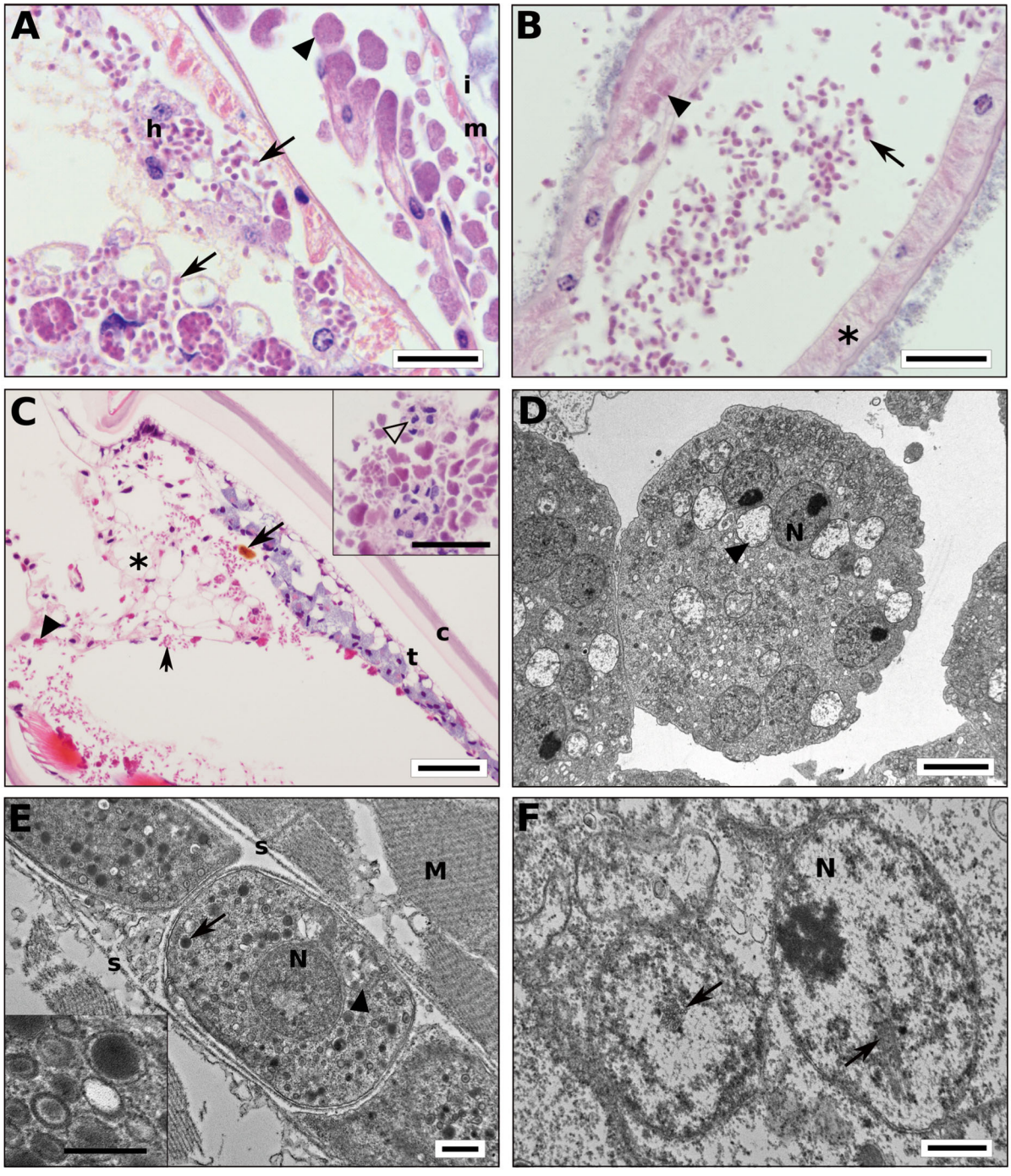

Fig. 2. Histological appearance and ultrastructure of *Haplosporidium echinogammari* infecting *Echinogammarus marinus* (MK913663; sampled in Newton's Cove 8 June 2016). (A) Unicellular stages found loose in the haemolymph (arrows) and within haemocytes (h). Plasmodial stages (arrowhead) filling the gap between the muscle layer (m) around the intestine (i) and the cardiac tissue. (B) Unicellular stages (monokaryotic and dikaryotic) within the haemal space (arrow) bounded by gill epithelium (*); also plasmodial stages (arrowhead) disrupting a gill epithelium cell. (C) Host-mediated response to infection includes melanization (long arrow) and granuloma formation (inset: transparent arrowhead). Host tissue disruption associated with unicellular stages (short arrow) and plasmodia (arrowhead) is patent in the connective (*) and tegument (t) which is associated with the carapace (c). (D) Transmission electron micrograph (TEM) of a plasmodial stage with at least 5 clear nuclei (N) and mitochondria (arrowhead). (E) TEM of a unicellular stage enveloped by host sarcolemma (s), interfering and substituting muscle fibres (M). A well-defined single nucleus (N), mitochondria (arrowhead) and haplosporosome-like structures (arrow and insertion) can be observed. (F) TEM of 2 ovoid electro-lucent nuclei (N) with peripheral compact chromatin, and microtubules (arrows). Scale bars = (A,B) 20 µm, (C) 50 µm (inset = 50 µm), (D) 2 µm, (E) 500 nm (inset = 250 µm), (F) 500 nm

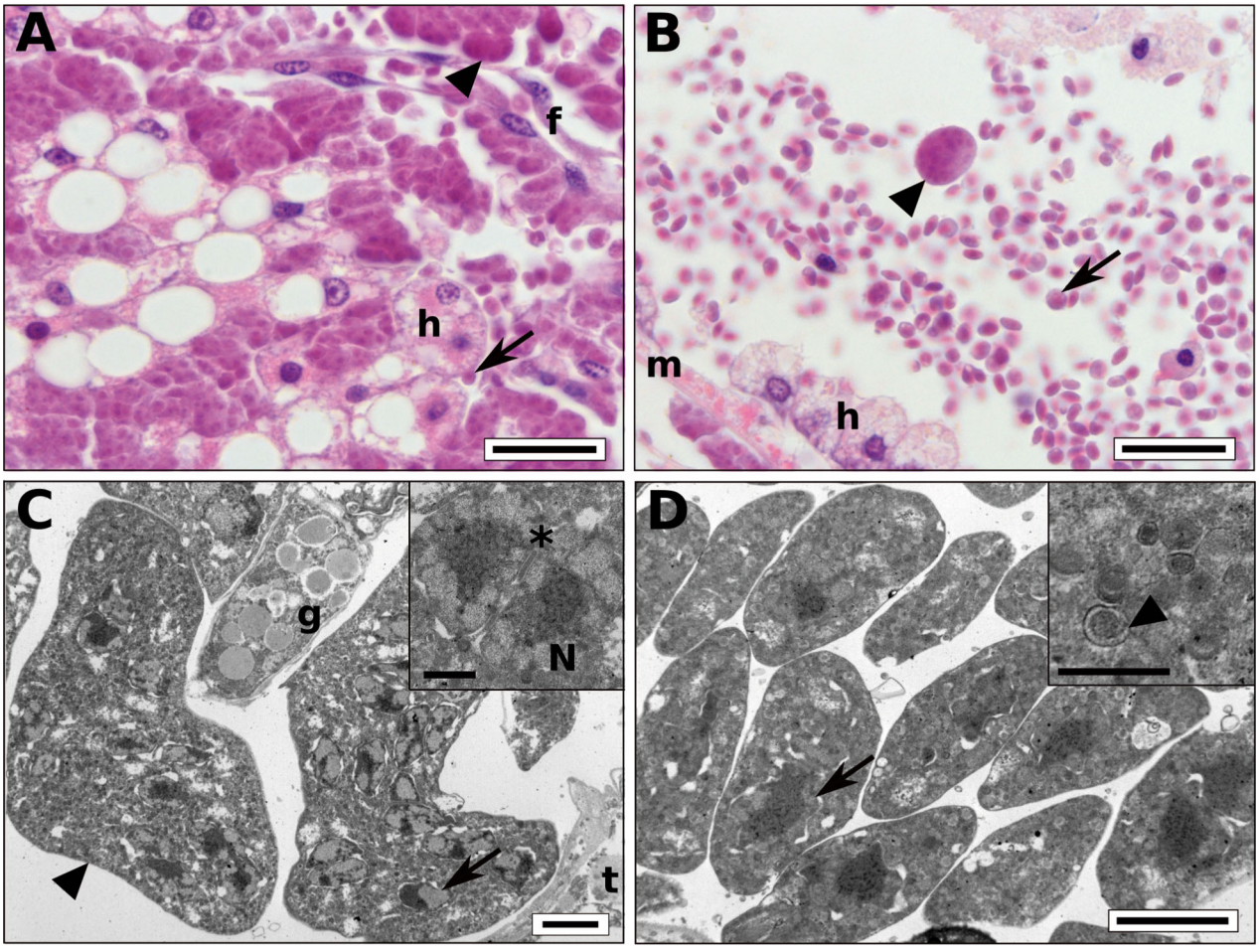

Fig. 3. Histological appearance and ultrastructure of *Haplosporidium orchestiae* infecting *Orchestia* sp. (MK913668; sampled in Dart estuary on 27 April 2017). (A) Congestion of the connective tissue around fibroblasts (f) and haemocytes (h), with plasmodial (arrowhead) and unicellular stages (arrow). (B) Monokaryotic and dikaryotic unicellular stages (arrow) and a single plasmodium (arrowhead) crowding the haemal sinus and sometimes within haemocytes (h) associated with the cardiac musculature (m). (C) TEM of 2 multinucleated plasmodia (arrowhead) within the haemal sinus of the host. A host granulocyte (g) and a fraction of disrupted tegument (t) can be observed. Inset: uneven nuclei with sparse chromatin (N) separated by an electron-dense cytokinetic structure (*). (D) TEM of unicellular stages of the parasite with 1 or 2 nuclei (arrow). Inset: detail of haplosporosome-like bodies (arrowhead). Scale bars = (A,B) 20 µm, (C,D) 2 µm (both insets = 500 nm)

brain and peripheral nervous system. In more intense infections, muscle and hepatopancreas were also affected, and occasionally, extended disruption of the intestine and tegument was present (Fig. 2C). In general, unicellular monokaryotic and dikaryotic stages of the parasite were found mainly in the haemolymph and to a lesser extent in the tegument, while plasmodial stages tended to congest the connective tissues around organs (Table 3). Chronic host response in the form of granuloma formation and melanization (Fig. 2C) in heavily infected individuals was observed. Haemocyte aggregations were noted for several infections regardless of the phase of the infection. In 15/17 selected amphipods (Table 3) there were sufficient (≥30) numbers of uncompressed plasmodia suitable for measurement. Sizes (mean ± SD) ranged from 6.6 ± 0.67 µm in parasite MK913655 infecting *E. marinus* in Newton's Cove in September 2016, to 9.4 ± 1.14 µm in parasite MK913668 infecting *Orchestia* sp. in the Dart estuary during April 2017.

Morphometric analysis of monokaryotic and dikaryotic stages shows 2 well defined groups within parasites infecting both host groups (Fig. 4). The length of the monokaryotic parasite cells (n = 30) infecting *E. marinus* ranged between 2.49 ± 0.29 and 2.79 ± 0.39 µm, and width between 1.64 and 1.78 ± 0.19 µm. Monokaryotic stages of the parasites infecting *Orchestia* sp. were consistently larger, with a minimum length of 3.46 µm and a maximum of 3.62 µm (SD between 0.24 and 0.44 µm) and width between 2.04 and 2.32 µm (SD between 0.15 and 0.36 µm; n = 30). There are clear differences in the size and shape of

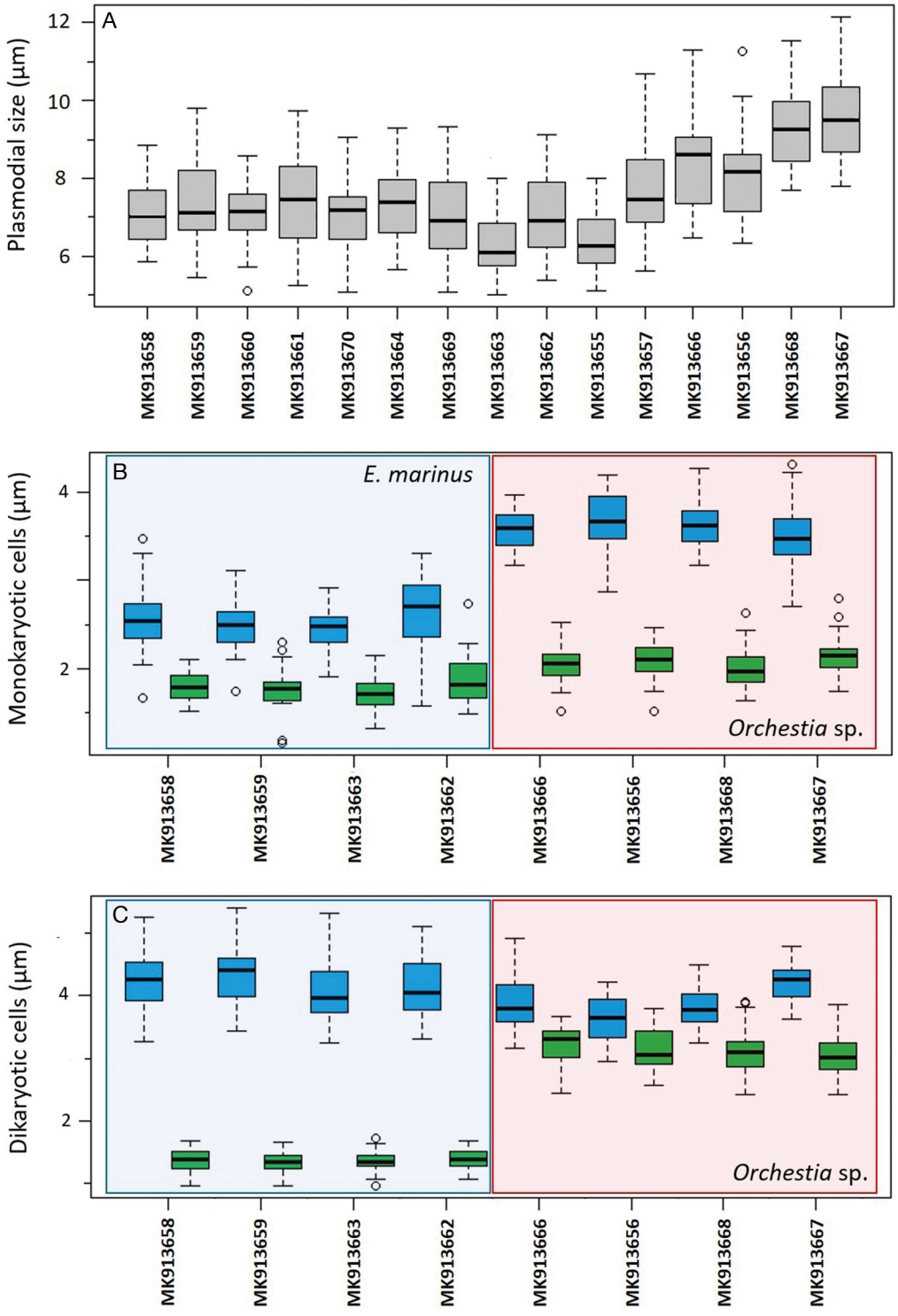

Fig. 4. Measurements (µm) of plasmodial and unicellular stages of each haplosporidian parasite against the infected hosts, showing the median (bar), 1st and 3rd quartiles (box), minimum and maximum (whiskers) and outliers (open circles). (A) Plasmodial stages for 15 hosts (see Table 3). Also shown are length (blue boxes) and width (green boxes) for (B) monokaryotic unicellular stages and (C) dikaryotic unicellular stages when present and measurable

dikaryotic stages of the 2 parasites. The elongated tube-like shape of cells in *E. marinus*, with a length ranging between 4.18 ± 0.31 and 4.72 ± 0.24 µm and a maximum width of 1.36 ± 0.12 µm (n = 30) contrast with the sub-spherical nature of the parasitic cells infecting *Orchestia* sp., which have a minimum width of 2.99 ± 0.28 µm and a length ranging between 3.51 and 3.97 µm (n = 30).

Ultrastructural differences between both groups (Figs. 2D–F & 3C,D) were evident in both unicellular and plasmodial stages. Plasmodial stages of the haplosporidian infecting *E. marinus* were more uniform, with slightly ovoid nuclei and small, very condensed peripheral nucleolus, and several mitochondria (Fig. 2D,F). In contrast, plasmodia of the parasite group infecting *Orchestia* sp. were more irregular and showed large nuclei with dispersed chromatin, and fewer mitochondria (Fig. 3C). Similarly, monokaryotic forms in *E. marinus* (Fig. 2E) possessed a central spherical nucleus, in an electron-lucent cytoplasm in which few clear mitochondria, electron dense vesicles, haplosporosome-like bodies and vesicles with 2 concentric membranes were observed (Fig. 2E). Unicellular cells infecting *Orchestia* sp. had an irregular central nucleus, with the chromatin widely distributed within a large amorphous nucleolus (Fig. 3C). No apparent mitochondria, and fewer haplosporosome-like bodies and double membrane vesicles in a more electron dense cytoplasm (Fig. 3D) were observed.

3.3. Molecular phylogeny

Haplosporidian SSU sequences (ca. 650 bp long, including the V9 region) were generated from 17 individual amphipods (Fig. 5). Clades I and II contained sequences from *Haplosporidium orchestiae* and *H. echinogammari*, respectively. Clade III was phylogenetically distinct from clade II, but was closely related to it. BlastN searches against GenBank revealed that sequences comprising the novel species *H. echinogammari* (Clade II) and Clade III were 97–98% similar to *H. diporeiae* (KF378734; 68% coverage) and 97–99% similar to environmental sequences KF208571 and KF208572 corresponding to haplosporidian clones 71 and 55, respectively (from water column and sediment samples from Weymouth and Italy).

The closest BlastN matches to *H. orchestiae* sequences were 93–94% similar (86% coverage) to uncultured Haplosporidian clone 29 (KF208579). However, Fig. 5 shows clone 53 (KF208574), sampled from the brackish waters of the Fleet lagoon (Weymouth) and marine waters of Newton's Cove, as the phylogenetically closest previously known relative of *H. orchestiae,* but there is no ML bootstrap or negligible Bayesian posterior probability (PP) support for the relationship. Although the branching position of *H. echinogammari* within lineage C (Hartikainen et al. 2014) is strongly supported, *H. orchestiae* is not strongly related to any previously known *Haplosporidium* lineage. The Polish freshwater amphipods were infected with both new *Haplosporidium* species. *H. orchestiae* infecting *G. varsoviensis* (MK913665) was 99.6% similar to that infecting *P. robustoides* (MK913664), and *H. echinogammari* infecting *P. robustoides* (MK913670 and MK913669) were 99.1 and 99% similar to MK913661 from Weymouth.

Within *H. echinogammari*, all amphipod-derived haplosporidian sequences were sampled from Newton's Cove between April and June in 2016 and 2017. MK913655 and MK913657, in Clade III, were collected in the same location in September and December 2016, respectively. *Orchestia* sp. was only observed and collected in Newton's Cove in September, but no haplosporidian infections were detected.

Phylogenetic analysis including sequences of haplosporidians amplified from other amphipods, isopods, crabs and crayfish (Fig. 6), none of which had matching histological or ultrastructural observations, showed that 22 out of 25 of these crustacean-derived sequences grouped within 3 main clades (Fig. 6). The reference codes and provenances of these sequences are shown in Table 4. Clade 1 included haplosporidians isolated from *Cancer pagurus* and *Carcinus maenas* incubations in artificial seawater, but also parasite-infected tissues from a crab sampled in Thailand, and from freshwater amphipods sampled in Florida (USA) and the UK. This clade also included lineages E and G from Hartikainen et al. (2014), the notorious oyster parasite *H. nelsoni* and *H. orchestiae*. However, there was negligible support for the whole clade. Clade 2 had less than 50% ML bootstrap and 0.92 Bayesian PP support, but comprised 2 more strongly supported clades, which corresponded to lineages F and B of Hartikainen et al. (2014), which did not branch together in the latter analysis. Prior to the present study, both B and F were represented by only 1 sequence each, B from a freshwater column, and F from water collected from the Fleet lagoon. Seven of our sequences, from isopods, crayfish, crabs and amphipods, grouped with B, and 3 (from amphipods and an isopod) grouped with F, all from brackish or freshwater sites. No non-crustacean hosts are currently known from Clade 2. Clade 3 (97/1.00), corresponding to lineage C of Hartikainen et al.

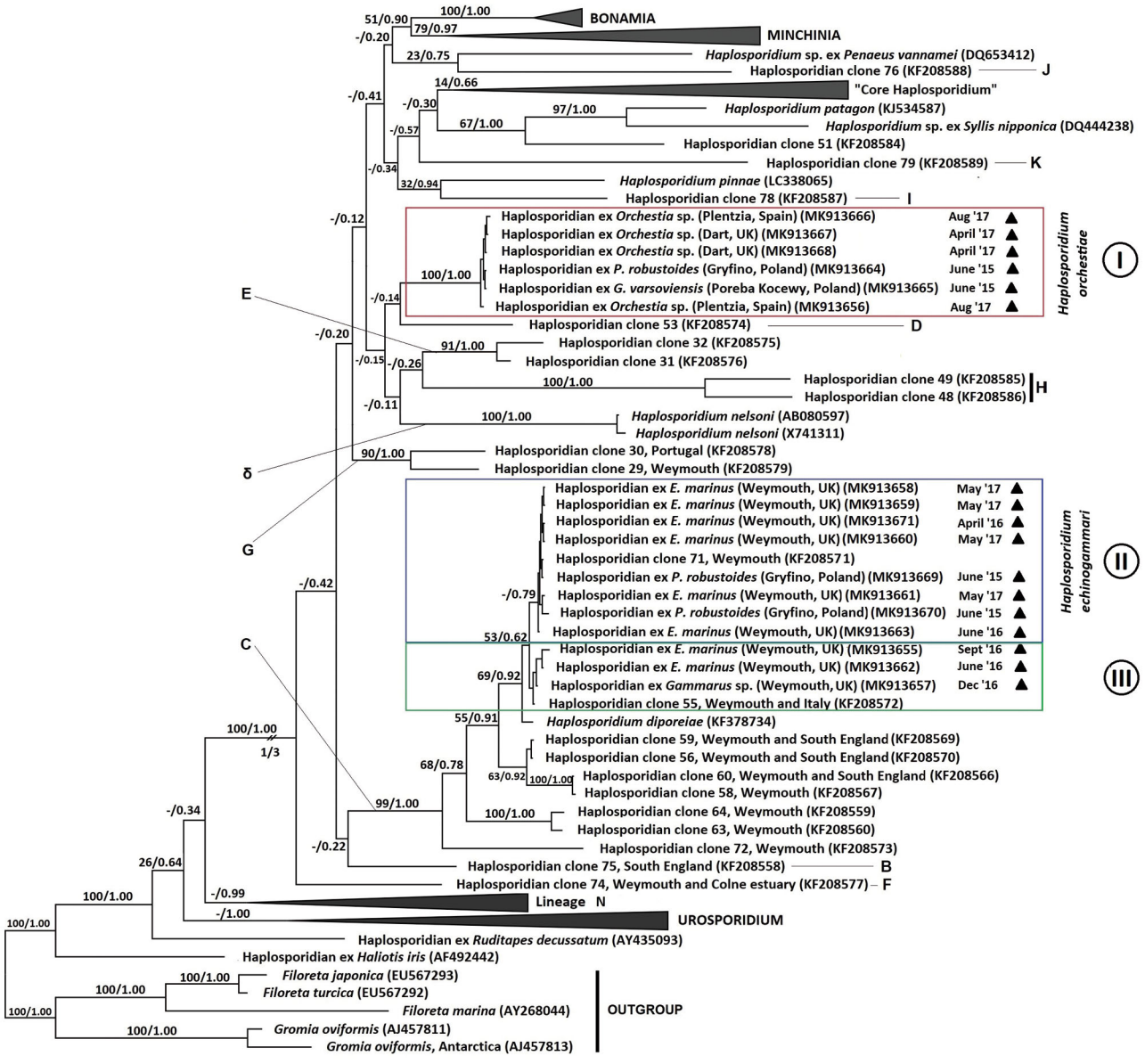

Fig. 5. Two novel haplosporidian species, *Haplosporidium orchestiae* and *H. echinogammari*, isolated from different amphipod species, in different locations, form 2 separate clades on the phylogenetic tree of the Haplosporida order. The consensus phylogenetic tree of the order was generated using Bayesian inference. Branches show posterior probabilities and bootstrap support from the maximum likelihood (ML) analysis. Black triangles mark those samples sequenced in this study. GenBank accession numbers are shown to the right of the parasite species or haplosporidian clone number. Circled Roman numerals indicate the 3 clades described in Section 3. Sequences belonging to *Bonamia* sp., *Minchinia* sp., 'Core' *Haplosporidium* sp., *Urosporidium* sp. and haplosporidian lineage 'N' associated with *Urosporidium* sp. have been collapsed. Lineages established by Hartikainen et al. (2014) are indicated with letters (B to K)

(2014), contained 9 novel sequence types generated in our study, 6 associated with crabs, and the rest with amphipods. In addition, this clade included *H. echinogammari* and *H. diporeiae*. All other previously known sequence types in this clade were either crustacean-associated or from water or sediment samples.

Only a few haplosporidian sequences from crustacean hosts branched outside of these clades. A haplosporidian sequence (Crab seq. 9) obtained from the incubation water of an individual of *C. pagurus* from Newton's Cove, branched robustly (87/0.99) as sister to *Urosporidium*, and was very similar to KF208597 from Newton's Cove water column (clone 90). Crab seq. 3, also from Newton's Cove *C. pagurus* incubation water, robustly branched within lineage N (97/1.00). The only haplosporidian sequence generated from amphipod tissues that did not group in any

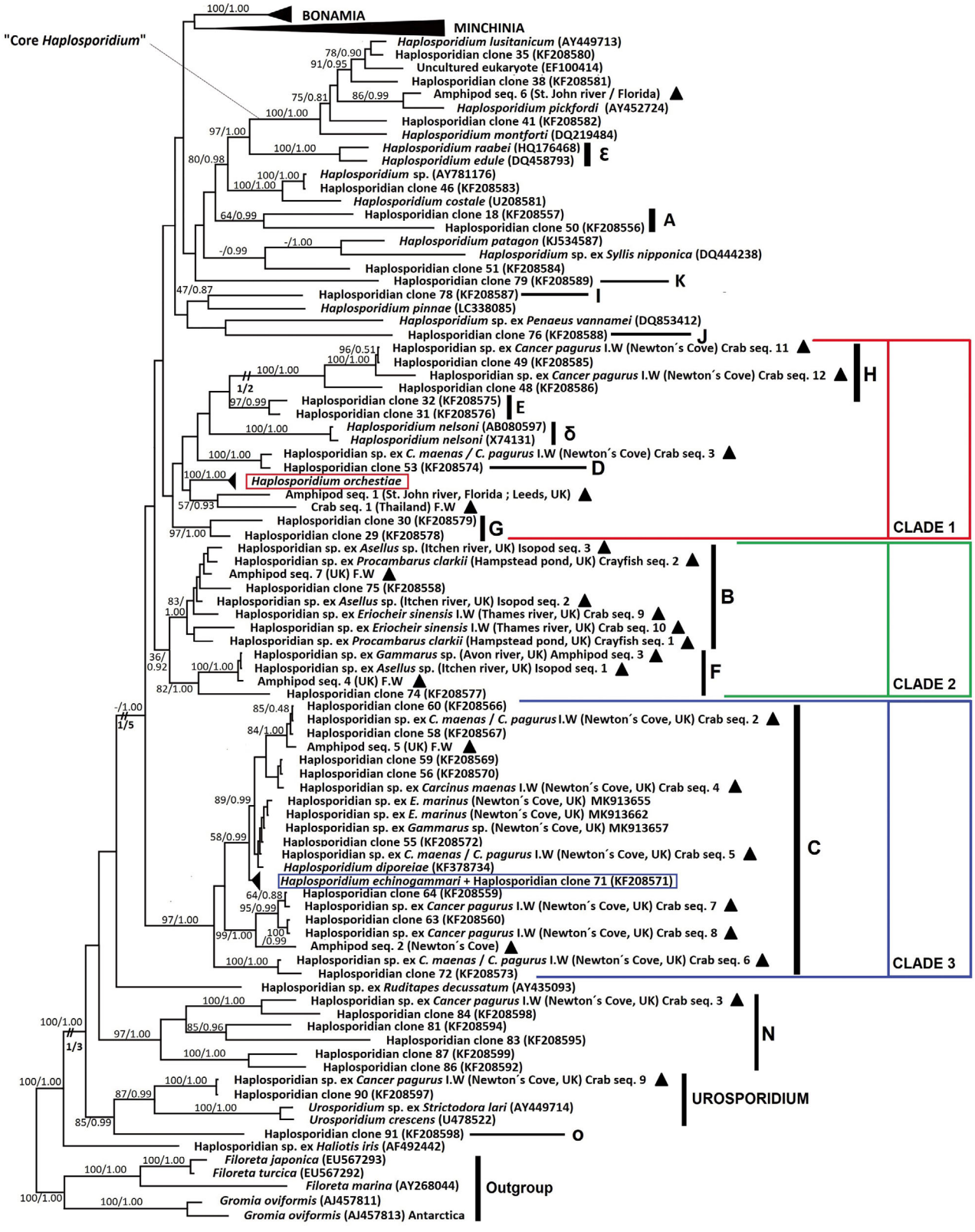

Fig. 6. Phylogenetic analysis demonstrates that most haplosporidian sequences associated with crustacean hosts group together in 3 clades. The consensus phylogenetic tree of the order Haplosporida was generated using Bayesian inference. Node support values of <75% (maximum likelihood bootstrap) and <0.85 (Bayesian posterior probability) are not shown. Where nodes are supported above either threshold, both values are given. Black triangles mark sequences associated with crustacean hosts included in the present study in addition to those of *H. echinogammari* and *H. orchestiae*. GenBank accession numbers are specified to the right of the parasite species or haplosporidian clone number. Sequences of *Bonamia* sp., and *Minchinia* sp. and groups of sequences forming *H. echinogammari* (blue rectangle) and *H. orchestiae* (red rectangle) included in Fig. 5 have been collapsed. Lineages established by Hartikainen et al. (2014) are indicated with letters (A to O)

of the 3 described crustacean clades was Amphipod seq. 6 from St John's River (Florida), which was sister to *H. pickfordi*, a parasite of freshwater snails, in the 'core' *Haplosporidium* clade.

3.4. Taxonomic summary

3.4.1. Novel species within existing lineage C (Hartikainen et al. 2014)

Sub-phylum: Endomyxa Cavalier-Smith, 2018
Class: Ascetosporea Cavalier-Smith, 2002
Order: Haplosporida Caullery & Mesnil, 1899
Family: Haplosporiidae Sprague, 1979
Genus: *Haplosporidium* Caullery & Mesnil, 1899
Species: *Haplosporidium echinogammari* sp. nov. Urrutia, Feist and Bass, 2018
Diagnosis: Spherical to elongated monokaryotic stages, with a length varying between 2.6 and 2.9 µm and a width around 1.7 ± 0.2 µm; they develop a more tubular shape when dikaryotic (length 4.5 ± 0.4 µm; width: 1.25 ± 0.2 µm). No sporulation observed. The plasmodia range in size between 6.6 and 8.02 µm in diameter, with no more than 20 nuclei per section. Infection develops in the connective tissue associated with digestive and tegumental glands, from where it spreads to other organs, eventually producing tissue disruption.
Type host: Amphipods (*Echinogammarus marinus*)
Type location: Coastal waters in Newton's Cove (UK)
Type material: Original slides used for this paper are stored together with biological material embedded in wax and epoxy resin in the Cefas Weymouth Lab. The type material is stored as RA 16046 (specimen no. 19), and the SSU rDNA sequence is deposited in GenBank under accession number MK913663.

3.4.2. Novel species within novel lineage

Sub-phylum: Endomyxa Cavalier-Smith, 2018
Class: Ascetosporea Cavalier-Smith, 2002
Order: Haplosporida Caullery & Mesnil, 1899
Family: Haplosporiidae Sprague, 1979. Genus: *Haplosporidium* Caullery & Mesnil, 1899
Species: *Haplosporidium orchestiae* sp. nov. Urrutia, Feist and Bass, 2018
Diagnosis: Spherical to elongated monokaryotic stages, with a length between 3.3 and 3.7 µm and a width around 2.2 ± 0.25 µm; become subspherical when dikaryotic (length 3.8 ± 0.3 µm; width 3.2 ± 0.2 µm). No sporulation observed. The plasmodia range in size between 7.81 and 9.4 µm in diameter, with no more than 15 nuclei per section. Infection develops in the connective tissue associated with digestive and tegumental glands, from where it spreads to other organs, eventually producing tissue disruption.
Type host: Amphipods (*Orchestia* sp.)
Type location: Estuarine waters in Dart (UK)
Type material: Original slides used for this paper are stored together with biological material embedded in wax and epoxy resin in Cefas Weymouth Lab. The type material is stored as RA17028 (specimen no. 47), and the SSU rDNA sequence is deposited in GenBank under accession MK913668.

4. DISCUSSION

Despite their ecological and economic importance, members of the order Haplosporida are understudied. The taxonomic relationships within the group remain a challenge more than a century after the discovery of the first species. Ecology, geographic distribution and biological cycle of most described species are poorly understood or unknown. The idea of a highly diverse order Haplosporida is not new. Previous phylogenetic studies (Reece et al. 2004, Hartikainen et al. 2014) have shown significant genetic diversity within the group and the likely paraphyly of the most species-rich genus, *Haplosporidium*. Hartikainen et al. (2014) published SSU rDNA sequences of 85 lineages, but only 48% of them have a known or suggested host. Of the remaining haplosporidian sequences, including 14 novel highly divergent lineages, 75% were from environmental samples (filtered water and/or sediment). Moreover, there is a need for host-based field surveys in order to characterize those clades and the species constituting them (Hartikainen et al. 2014). Our histopathological survey of prominent invertebrate groups in coastal ecosystems in the south of England showed amphipods to be frequently infected by haplosporidian parasites. While the *H. orchestiae* type sequence did not match with any of the environmental sequences in Hartikainen et al. (2014), the *H. echinogammari* type sequence (MK913663) was almost identical to KF208571 collected from the water column in Newton's Cove. Moreover, it was closely related to KF208572 and other sequences within Lineage C (KF208566, KF208567, KF208569, KF208570) found in the water column and the sediment at the same location.

Morphological discrimination of haplosporidians is often based on characterization of the spore orna-

Table 4. Novel haplosporidian sequences obtained from parasites associated with crustacean hosts included in Fig. 6. The reference used for each sequence in the phylogenetic tree (Fig. 6) is related to the host species if known, the sampling location and year of collection, and whether the sample was obtained from infected tissue or from the filter after incubation in artificial seawater

Crustacean taxon	Sequence reference	Host species	Sampling location	Tissue infection / Incubation water
Order Amphipoda	Amphipod seq. 1	Unknown	St. John river (Florida); Leeds (UK)	Tissue
	Amphipod seq. 2	Unknown	Newton's Cove (UK)	Tissue
	Amphipod seq. 3	*Gammarus* sp.	River Avon (UK)	Tissue
	Amphipod seq. 4	Unknown	Fresh water environment (UK)	Tissue
	Amphipod seq. 5	Unknown	Fresh water environment (UK)	Tissue
	Amphipod seq. 6	Unknown	St. John river (Florida)	Tissue
	Amphipod seq. 7	Unknown	Fresh water environment (UK)	Tissue
Order Isopoda	Isopod seq. 1	*Asellus* sp.	River Avon (UK)	Tissue
	Isopod seq. 2	*Asellus* sp.	River Itchen (UK)	Tissue
	Isopod seq. 3	*Asellus* sp.	River Itchen (UK)	Tissue
Order Decapoda	Crab seq. 1	Unknown	Fresh water environment (Thailand)	Tissue
	Crab seq. 2	*C. pagurus* and *C. maenas*	Newton's Cove (UK) 2013	Incubation water
	Crab seq. 3	*C. pagurus* and *C. maenas*	Newton's Cove (UK) 2013	Incubation water
	Crab seq. 4	*Carcinus maenas*	Newton's Cove (UK) 2013	Incubation water
	Crab seq. 5	*C. pagurus* and *C. maenas*	Newton's Cove (UK) 2013	Incubation water
	Crab seq. 6	*C. pagurus* and *C. maenas*	Newton's Cove (UK) 2013	Incubation water
	Crab seq. 7	*Cancer pagurus*	Newton's Cove (UK) 2013	Incubation water
	Crab seq. 8	*Cancer pagurus*	Newton's Cove (UK) 2013	Incubation water
	Crab seq. 9	*Eriocheir sinensis*	River Thames (UK) 2014	Incubation water
	Crab seq. 10	*Eriocheir sinensis*	River Thames (UK) 2014	Incubation water
	Crab seq. 11	*Cancer pagurus*	Newton's Cove (UK) 2013	Incubation water
	Crab seq. 12	*Cancer pagurus*	Newton's Cove (UK) 2013	Incubation water
	Crayfish seq. 1	*Procambarus clarkii*	Hampstead Head, Pond (UK) 2015	Tissue
	Crayfish seq. 2	*Procambarus clarkii*	Hampstead Head, Pond (UK) 2015	Tissue

mentation, size and ontogeny of the spore (Perkins 2000, Burreson & Reece 2006). Interestingly, in contrast to sporogenesis of *H. diporeiae* in the amphipod genus *Diporeia*, which was observed to occur synchronously with continued plasmodial development (Messick 2009, Winters & Faisal 2014), we detected no sporogonic stages or mature spores in our samples (n = 64), despite sampling over 2 infection cycles of *H. echinogammari* at least, and our samples representing a range of infection stages. The absence of spores in our samples may have (one of) several explanations, including sporogenesis occurring only under certain conditions that were not met in our samples, the infection cycle completing without spores being produced, sporogenesis taking place in other host species, or simply because our sampling missed the sporulating stages. However, efforts to find alternate hosts in the life cycle of *H. echinogammari* and *H. orchestiae* have been unsuccessful. The fate of spores after they are released from the host remains unknown, even for the best studied haplosporidian, *H. nelsoni* (Carnegie & Burreson 2012). In *H. orchestiae* and *H. echinogammari*, initial infection is observed in tissues directly exposed to the environment, primarily tegument and gills, but also in the connective tissue around the intestine, leaving open several possibilities as the portal of infection.

Description of spore morphology is not an essential requirement for the description of protistan parasite taxa when other phenotypic and phylogenetic characteristics are considered together. In the case of the 2 new species described here, morphological features of the plasmodial and unicellular stages present in *Orchestia* sp. and *Echinogammarus* sp. were sufficient to differentiate the parasites. Morphological, including ultrastructural, and phylogenetic differences between *H. orchestiae* and *H. echinogammari* clearly define them as distinct taxa. The phylogenetic relationships of *H. orchestiae* to existing uncharacterized lineages (D, E, H and δ) described by Hartikainen et al. (2014) are unresolved, and it is clearly distinct from the apparently closest related characterized species, *H. nelsoni* (Haskin et al. 1966). *H. echinogammari* is more closely related to a previously characterized species, *H. diporeiae*, but is distinguished from it phylogenetically, and perhaps by

spore-forming propensity. There are insufficient data available to determine whether *H. echinogammari* can be distinguished from *H. diporeiae* on the basis of ultrastructure or histological appearance.

Since the evolutionary distance between Haplosporidian clone 71 (KF208571), collected from Weymouth in 2012 (Hartikainen et al. 2014), and *H. echinogammari* was smaller than the distance between some of the sequences within the clade, clone 71 was reassigned as *H. echinogammari*. Not all of the haplosporidians infecting *E. marinus* are classified as *H. echinogammari*. Clade III in Fig. 5, which includes parasites sampled from the same host and location (Newton's Cove), is formed by 2 haplosporidians infecting *Gammarus* and *Echinogammarus*, plus Haplosporidian clone 55 (KF208572) isolated from Newton's Cove and a freshwater system in Italy. Clade III is phylogenetically distinct from clade II, but because morphology and histopathology of the parasites examined from clade III were indistinguishable from those of clade II, and no ultrastructural data are available for clade III, there is insufficient evidence to classify clade III as either *H. echinogammari* or a different novel species. Future work based on larger sample numbers may justify its separate description. We note that, in contrast to *H. echinogammari* which appears to infect *E. marinus* in late spring (May and June), this second group of parasites is responsible for infections developed during more varied times of the year, suggesting a potential role for seasonality in discriminating between these lineages.

Only 2 further amphipod species have previously been found to harbour haplosporidian infections: *Rivulogammarus pulex* and *Parhyale hawaiensis*, the first from freshwater systems in Belgium and Sweden (Van Ryckeghem 1930, Larsson 1987), and the second from the Egyptian coast of the Red Sea (Ismail 2011). No genetic sequence data are available for either parasite, and ultrastructural comparison is difficult due to the lack of similar stages presented in the studies. Lineage C (Hartikainen et al. 2014) was presented as a highly diverse group with a clear preference for estuarine and rocky shore locations. While 40% of the sequences within the clade are currently uncharacterized, the remainder derives from different species of amphipods sampled from diverse aquatic environments. We suggest that evolutionary diversification of haplosporidians within lineage C might in future be related to amphipod host specificity and/or seasonality, a feature proposed for other parasite groups (Lange et al. 2015, González-Tortuero et al. 2016).

While molluscs may be the most diverse hosts for haplosporidian parasites, crustaceans are increasingly reported as hosts (Stentiford et al. 2013), including infections affecting commercial species (Bower & Meyer 2002, Utari et al. 2012). However, crustacean-derived haplosporidians have so far appeared to branch without discernible pattern among mollusc-infecting lineages. For instance, *H. littoralis* infecting crabs is included within the 'core' *Haplosporidium* group, which includes well-known parasites of oysters, mussels, cockles and snails (*H. costale*, *H. pickfordi*, *H. edule*, *H. montforti*, *H. raabei*), while the haplosporidian infecting shrimp *Pennaeus vannamei* (Dyková et al. 1988, Nunan et al. 2007) is related to uncharacterized lineages F and G, *H. diporeiae* to the recently characterized amphipod-infecting lineage C, and *H. louisiana* is close to trematode-infecting *Urosporidium* sp. The phylogenetic analyses in this paper include 25 novel sequences of haplosporidians either infecting or associated with crustacean hosts, 92% of which group together in 3 crustacean-rich clades. Clade 1 includes *H. nelsoni* and lineages D, E, G and H, originally described by Hartikainen et al. (2014), to which this study adds *H. orchestiae*. Support for this clade is extremely weak, although it contains several strongly supported clades: the long-branched H is so far only associated with crustaceans as putative hosts, as is D, and novel lineages detected in this study (Fig. 6). The haplosporidians detected in crab incubation water experiments suggest that crabs are hosts or/and vectors of these parasites.

In clade 2, we show that lineages B and F of Hartikainen et al. (2014) are also dominated by crustacean-associated haplosporidians from brackish and freshwater habitats. No mollusc-associated haplosporidians have yet been detected in these clades, although non-marine mollusc hosts have not been sampled anywhere near as intensively as our screening of potential crustacean hosts in this study, and marine molluscs previously. Of additional interest is our finding that, with the increased taxon sampling from the present study, lineages B and F are grouping together, albeit relatively weakly, which was not the case in Hartikainen et al. (2014). In clade 3 (lineage C of Hartikainen et al. 2014), amphipod-derived parasite lineages are often closely related to those amplified from crabs. This might indicate some correspondence between crab and amphipod parasites. Perhaps their life cycles involve both hosts, there are relatively easy evolutionary transitions between crab and amphipods as main hosts, or their detection in crabs derives from infected amphipods being consumed by crabs. A dedicated investigation of crab-infecting haplosporidians at the same site

would clarify this. However, it is noteworthy that the 2 new *Haplosporidium* species described in this paper have only ever been amplified from amphipod tissue or, and only in the case of *H. echinogammari*, host-independent environmental samples.

Acknowledgements. A.U. was supported by a PhD studentship grant (Programa Predoctoral de Formación de Personal Investigador - Departamento Educación Gobierno Vasco); the experimental work was funded by the UK Department of Environment, Food and Rural Affairs (Defra) under contracts FC1214 (to D.B.) and FB002A (to S.W.F. and D.B.). We thank Matt Green, Corey Holt, Chantelle Hooper, Rose Kerr, Robert McFarling, John Bignell, Catherine Troman, Caroline Daumich, Kelly Bateman and Grant Stentiford, who assisted with sample collection and processing and provided advice.

LITERATURE CITED

Bancroft JD, Cook HC (1994) Manual of histological techniques and their diagnostic application. Churchill Livingstone, New York, NY

Berthe FC, Le Roux F, Peyretaillade E, Peyret P, Rodriguez D, Gouy M, Vivarès CP (2000) Phylogenetic analysis of the small subunit ribosomal RNA of *Marteilia refringens* validates the existence of Phylum Paramyxea. J Eukaryot Microbiol 47:288–293

Bocher P, Cherel Y, Labat JP, Mayzaud P, Razouls S, Jouventin P (2001) Amphipod-based food web: *Themisto gaudichaudii* caught in nets and by seabirds in Kerguelen waters, southern Indian Ocean. Mar Ecol Prog Ser 223:261–276

Bojko J (2017) Parasites of invasive Crustacea: risks and opportunities for control. PhD dissertation, University of Leeds

Bower SM, Meyer GR (2002) Morphology and ultrastructure of a protistan pathogen in the haemolymph of shrimp (*Pandalus* spp.) in the northeastern Pacific Ocean. Can J Zool 80:1055–1068

Burreson EM, Ford SE (2004) A review of recent information on the Haplosporidia, with special reference to *Haplosporidium nelsoni* (MSX disease). Aquat Living Resour 17:499–517

Burreson EM, Reece KS (2006) Spore ornamentation of *Haplosporidium nelsoni* and *Haplosporidium costale* (Haplosporidia), and incongruence of molecular phylogeny and spore ornamentation in the Haplosporidia. J Parasitol 92:1295–1301

Carnegie RB, Burreson EM (2012) *Perkinsus marinus* and *Haplosporidium nelsoni*. In: Woo PTK, Buchmann K (eds) Fish parasites: pathobiology and protection. CABI Publishing, Wallingford, p 92–108

Carnegie RB, Burreson EM, Hine P, Stokes NA, Audemard C, Bishop MJ, Peterson CH (2006) *Bonamia perspora* n. sp. (Haplosporidia), a parasite of the oyster *Ostreola equestris*, is the first *Bonamia* species known to produce spores. J Eukaryot Microbiol 53:232–245

Catanese G, Grau A, Valencia JM, Garcia-March JR and others (2018) *Haplosporidium pinnae* sp. nov., a haplosporidan parasite associated with mass mortalities of the fan mussel, *Pinna nobilis*, in the Western Mediterranean Sea. J Invertebr Pathol 157:9–24

Caullery M, Mesnil F (1899) Sur le genre *Aplosporidium* (nov) et l'ordre nouveau des Aplosporidies. CR Seances Soc Biol Paris 51:789–791

Cavalier-Smith T (1993) Kingdom Protozoa and its 18 phyla. Microbiol Rev 57:953–994

Cave CS, Strychar K (2015) Decline of *Diporeia* in Lake Michigan: Was disease associated with invasive species the primary factor? Int J Biol 7:93–99

Chomczynski P, Sacchi N (1987) Single-step method of RNA isolation by acid guanidinium thiocyanate-phenol-chloroform extraction. Anal Biochem 162:156–159

Dyková I, Lom J, Fajer E (1988) A new haplosporean infecting the hepatopancreas in the penaeid shrimp, *Penaeus vannamei.* J Fish Dis 11:15–22

Fialkowski W, Fialkowska E, Smith BD, Rainbow PS (2003) Biomonitoring survey of trace metal pollution in streams of a catchment draining a zinc and lead mining area of Upper Silesia, Poland using the amphipod *Gammarus fossarum.* Int Rev Hydrobiol 88:187–200

Ford SE, Figueras AJ (1988) Effects of sublethal infection by the parasite *Haplosporidium nelsoni* (MSX) on gametogenesis, spawning, and sex ratios of oysters in Delaware Bay, USA. Dis Aquat Org 4:121–133

Ford SE, Tripp MR (1996) Diseases and defense mechanisms. In: Newell RIE, Kennedy VS, Eble AF (eds) The eastern oyster *Crassostrea virginica*. Maryland Sea Grant College, Cambridge, MD, p 383–450

Friedman CS, Perkins FO (1994) Range extension of *Bonamia ostreae* to Maine, USA. J Invertebr Pathol 64:179–181

Garrison LP, Link JS (2000) Dietary guild structure of the fish community in the Northeast United States continental shelf ecosystem. Mar Ecol Prog Ser 202:231–240

González-Tortuero E, Rusek J, Turko P, Petrusek A and others (2016) *Daphnia* parasite dynamics across multiple *Caullerya* epidemics indicate selection against common parasite genotypes. Zoology 119: 314–321

Hanna SK, Miller RJ, Zhou D, Keller AA, Lenihan HS (2013) Accumulation and toxicity of metal oxide nanoparticles in a soft-sediment estuarine amphipod. Aquat Toxicol 142:441–446

Hartikainen H, Ashford OS, Berney C, Okamura B and others (2014) Lineage-specific molecular probing reveals novel diversity and ecological partitioning of haplosporidians. ISME J 8:177–186

Haskin HH, Andrews JD (1988) Uncertainties and speculations about the life cycle of the eastern oyster pathogen *Haplosporidium nelsoni* (MSX). In: Fisher WS (ed) Disease processes in marine bivalve molluscs. Special Publication 18. American Fisheries Society, Bethesda, MD, p 5–22

Haskin HH, Stauber LA, Mackin JA (1966) *Minchinia nelsoni* n. sp. (Haplosporida, Haplosporidiidae): causative agent of the Delaware Bay oyster epizoötic. Science 153: 1414–1416

Hine PM, Carnegie RB, Burreson EM, Engelsma MY (2009) Inter-relationships of haplosporidians deduced from ultrastructural studies. Dis Aquat Org 83:247–256

Holst M, Stirling I, Hobson KA (2001) Diet of ringed seals (*Phoca hispida*) on the east and west sides of the North Water Polynya, northern Baffin Bay. Mar Mamm Sci 17: 888–908

Hopwood D (1996) Fixation and fixatives. In: Bancroft JD, Steven A, Turner DR (eds) Theory and practice of histological techniques. Churchill Livingstone, New York, NY, p 29–42

Ismail TG (2011) Coexistence of two species of haplosporidian parasites in a population of the marine amphipod *Parhyale hawaiensis* with evidence for parasite phagocytosis and transmission mode. J Egypt Soc Parasitol 41: 227–241

Katoh K, Rozewicki J, Yamada KD (2017) MAFFT online service: multiple sequence alignment, interactive sequence choice and visualization. Brief Bioinform 2017:bbx108

Kozlov AM, Darriba D, Flouri T, Morel B, Stamatakis A (2019) RAxML-NG: a fast, scalable, and user-friendly tool for maximum likelihood phylogenetic inference. Bioinformatics 2019:btz305

Kumar S, Stecher G, Tamura K (2016) MEGA7: molecular evolutionary genetics analysis version 7.0 for bigger datasets. Mol Biol Evol 33:1870–1874

Lange B, Kaufmann AP, Ebert D (2015) Genetic, ecological and geographic covariables explaining host range and specificity of a microsporidian parasite. J Anim Ecol 84: 1711–1719

Larsson A (2014) AliView: a fast and lightweight alignment viewer and editor for large datasets. Bioinformatics 30: 3276–3278

Larsson JIR (1987) On *Haplosporidium gammari*, a parasite of the amphipod *Rivulogammarus pulex*, and its relationships with the phylum Ascetospora. J Invertebr Pathol 49:159–169

MacNeil C, Dick JT, Elwood RW (1997) The trophic ecology of freshwater Gammarus spp. (Crustacea: Amphipoda): problems and perspectives concerning the functional feeding group concept. Biol Rev Camb Philos Soc 72: 349–364

Messick GA (2009) Haplosporidian parasite in *Diporeia* spp. amphipods from the Great Lakes region, USA. Dis Aquat Org 83:153–157

Miller MA, Pfeiffer W, Schwartz T (2010) Creating the CIPRES Science Gateway for inference of large phylogenetic trees. In: Gateway Computing Environments Workshop (GCE), IEEE, Piscataway, NJ, p 1–8

Moren M, Malde MK, Olsen RE, Hemre GI, Dahl L, Karlsen Ø, Julshamn K (2007) Fluorine accumulation in Atlantic salmon (*Salmo salar*), Atlantic cod (*Gadus morhua*), rainbow trout (*Onchorhyncus* [sic] *mykiss*) and Atlantic halibut (*Hippoglossus hippoglossus*) fed diets with krill or amphipod meals and fish meal-based diets with sodium fluoride (NaF) inclusion. Aquaculture 269:525–531

Nalepa TF, Fanslow DL, Pothoven SA, Foley AJ, Lang GA (2007) Long-term trends in benthic macroinvertebrate populations in Lake Huron over the past four decades. J Gt Lakes Res 33:421–436

Norderhaug KM, Christie H (2011) Secondary production in a *Laminaria hyperborea* kelp forest and variation according to wave exposure. Estuar Coast Shelf Sci 95:135–144

Nunan LM, Lightner DV, Pantoja CR, Stokes NA, Reece KS (2007) Characterization of a rediscovered haplosporidian parasite from cultured *Penaeus vannamei*. Dis Aquat Org 74:67–75

Ormières R (1980) *Haplosporidium parisi* n. sp., haplosporidian parasite of *Serpula vermicularis*. Ultrastructural study of the spore. Protistologica 16:467–474

Paramor OAL, Hughes RG (2004) The effects of bioturbation and herbivory by the polychaete *Nereis diversicolor* on loss of saltmarsh in south east England. J Appl Ecol 41: 449–463

Perkins FO (2000) Phylum Haplosporidia. In: Lee JJ, Leedale GF, Bradbury P (eds) An illustrated guide to the Protozoa, Vol 2. Society of Protozoologists/Allen Press, Lawrence, KS, p 1328–1341

Pichot Y, Comps M, Tige G, Grizel H, Rabouin MA (1979) Recherches sur *Bonamia ostreae* gen. n., sp. n., parasite nouveau de l'huître plate *Ostrea edulis*. Rev Trav Inst Peches Marit 43:131–140

Poltermann M (2001) Arctic sea ice as feeding ground for amphipods – food sources and strategies. Polar Biol 24: 89–96

Rambaut A (2014) FigTree, tree figure drawing tool. v. 1.4. 2. Institute of Evolutionary Biology, University of Edinburgh. http://tree.bio.ed.ac.uk (accessed 28 Nov 2018).

Reece KS, Siddall ME, Stokes NA, Burreson EM (2004) Molecular phylogeny of the Haplosporidia based on two independent gene sequences. J Parasitol 90:1111–1122

Reynolds ES (1963) The use of lead citrate at high pH as an electron-opaque stain in electron microscopy. J Cell Biol 17:208–212

Ronquist F, Teslenko M, Van Der Mark P, Ayres DL and others (2012) MrBayes 3.2: efficient Bayesian phylogenetic inference and model choice across a large model space. Syst Biol 61:539–542

Sheader M, Van Dover CL, Thurston MH (2004) Reproductive ecology of *Bouvierella curtirama* (Amphipoda: Eusiridae) from chemically distinct vents in the Lucky Strike vent field, Mid-Atlantic Ridge. Mar Biol 144:503–514

Stentiford GD, Bateman KS, Stokes NA, Carnegie RB (2013) *Haplosporidium littoralis* sp. nov.: a crustacean pathogen within the Haplosporida (Cercozoa, Ascetosporea). Dis Aquat Org 105:243–252

Trigos S, García-March JR, Vicente N, Tena J, Torres J (2014) Utilization of muddy detritus as organic matter source by the fan mussel *Pinna nobilis*. Mediterr Mar Sci 15:667–674

Utari HB, Senapin S, Jaengsanong C, Flegel TW, Kruatrachue M (2012) A haplosporidian parasite associated with high mortality and slow growth in *Penaeus* (*Litopenaeus*) *vannamei* cultured in Indonesia. Aquaculture 366-367: 85–89

Van Ryckeghem J (1930) Les Cnidosporidies et autres parasites du *Gammarus pulex*. Cellule 39:400–416

Ward GM, Neuhauser S, Groben R, Ciaghi S, Berney C, Romac S, Bass D (2018) Environmental sequencing fills the gap between parasitic haplosporidians and free living giant amoebae. J Eukaryot Microbiol 65:574–586

Wilson EE, Wolkovich EM (2011) Scavenging: how carnivores and carrion structure communities. Trends Ecol Evol 26:129–135

Winters AD, Faisal M (2014) Molecular and ultrastructural characterization of *Haplosporidium diporeiae* n. sp., a parasite of *Diporeia* sp. (Amphipoda, Gammaridea) in the Laurentian Great Lakes (USA). Parasit Vectors 7:343

Zhang Z, Schwartz S, Wagner L, Miller W (2000) A greedy algorithm for aligning DNA sequences. J Comput Biol 7: 203–214

Editorial responsibility: Jeffrey Shields, Gloucester Point, Virginia, USA

Submitted: December 10, 2018; Accepted: August 28, 2019
Proofs received from author(s): October 2, 2019